Amino Acid Substitutions at Positions 207 and 221 Contribute to Catalytic Differences between Murine Glutathione *S*-Transferase Al-1 and A2-2 toward (+)-*anti*-7,8-Dihydroxy-9,10-epoxy-7,8,9,10-tetrahydrobenzo[*a*]pyrene[†,‡]

Hong Xia,[§] Yijun Gu,[§,||] Su-Shu Pan,[⊥] Xinhua Ji,[||] and Shivendra V. Singh*[,§]

Cancer Research Laboratory, Mercy Hospital of Pittsburgh, Pittsburgh, Pennsylvania 15219, Pittsburgh Cancer Institute, University of Pittsburgh Medical Center, Pittsburgh, Pennsylvania 15213, and ABL-Basic Research Program, National Cancer Institute-Frederick Cancer Research and Development Center, Frederick, Maryland 21702

Received April 7, 1999; Revised Manuscript Received June 10, 1999

ABSTRACT: We have previously identified a novel Alpha class murine glutathione (GSH) *S*-transferase isoenzyme (designated mGSTAl-2) which is exceptionally efficient in catalyzing the GSH conjugation of (+)-*anti*-7,8-dihydroxy-9,10-epoxy-7,8,9,10-tetrahydrobenzo[*a*]pyrene [(+)-*anti*-BPDE], the ultimate carcinogen of widespread environmental pollutant benzo[*a*]pyrene. Furthermore, we have demonstrated that the Al-type subunit of this isoenzyme is significantly more active toward (+)-*anti*-BPDE than the other subunit (mGSTA2). To establish the basis for catalytic differences between mGSTAl and mGSTA2, which differ in their primary structures by 10 amino acids [distributed in three sections (I−III) as clusters of two (residues 65 and 95), three (residues 157, 162, and 169), and five (residues 207, 213, 218, 221, and 222) amino acids], three chimeric enzymes were expressed and tested for their activity toward (+)-*anti*-BPDE. These studies revealed that amino acid substitution(s) in section III determined the high catalytic activity of mGSTAl. Molecular modeling studies suggested that amino acid substitutions at positions 207 and/or 221, but not at positions 213, 218, and 222, may be responsible for such a difference. To test this possibility, amino acids at positions 207 and 221 of mGSTAl were mutated with the equivalent residues of mGSTA2. Kinetic analysis of the wild type and the mutant enzymes revealed that both methionine-207 and isoleucine-221 are critical for higher activity of mGSTA1-1 toward (+)-*anti*-BPDE compared with that of mGSTA2-2.

Benzo[*a*]pyrene (BP)[1] is the prototypical and best-characterized member of the polycyclic aromatic hydrocarbon (PAH) family of environmental pollutants, which are suspected human carcinogens (*1*). The tumorigenic activity of BP is attributed to its metabolite (+)-*anti*-7,8-dihydroxy-9,10-epoxy-7,8,9,10-tetrahydrobenzo[*a*]pyrene [(+)-*anti*-BPDE] (*2*, *3*), which is formed through catalysis by cytochrome P450-dependent monooxygenases and epoxide hydrolase (*4*−*6*). Covalent interaction of the epoxide function of (+)-*anti*-BPDE with nucleophilic centers in DNA is believed to be a crucial event in BP-induced tumorigenesis (*7*). Several different mechanisms have been identified which can inactivate (+)-*anti*-BPDE and, therefore, reduce its level of interaction with DNA. The known mechanisms of (+)-*anti*-BPDE inactivation include spontaneous hydrolysis to tetrols and ketodiols, nonenzymatic as well as cytochrome P450-catalyzed conversion to triols and triolepoxides, hydration by epoxide hydrolase, and glutathione (GSH) *S*-transferase (GST)-catalyzed conjugation with GSH (*8*−*13*). However, GST-catalyzed conjugation of (+)-*anti*-BPDE with GSH is believed to be the most important mechanism of its cellular detoxification (*11*−*13*). Thus, it has been shown that purified cytosolic rat liver GST isoenzymes reduce the level of binding of BPDE to DNA (*14*), and that overexpression of GSTs in cells, through stable transfection, reduces the level of BPDE−DNA adduct formation (*15*, *16*).

GST constitutes a superfamily of multifunctional isoenzymes which can catalyze the addition of GSH to electrophilic centers in a wide variety of endogenous and exogenous compounds (*17*, *18*). The cytosolic GST activity in mammalian tissues is often expressed by multiple isoenzymes, which arise from dimeric combinations of identical (homodimer) or nonidentical subunits (heterodimer) (*17*, *18*). On the basis of amino acid sequence homology, immunological cross-reactivity, and substrate specificity, mammalian cytosolic GSTs have been grouped into at least seven

[†] This investigation was supported in part by U.S. Public Health Service Grant RO1 CA76348 (S.V.S.), awarded by the National Cancer Institute (NCI), and by the NCI, Department of Health and Human Services (DHHS), under contract with ABL (X.J.).

[‡] The contents of this publication do not necessarily reflect the views or policies of the DHHS, nor does mention of trade names, commercial products, or organizations imply endorsement by DHHS or the United States Government.

* Corresponding author. Fax: (412) 232-5753. E-mail: ssingh@mercy.pmhs.org.

[§] Mercy Hospital of Pittsburgh.

[||] National Cancer Institute-Frederick Cancer Research and Development Center.

[⊥] University of Pittsburgh Medical Center.

[1] Abbreviations: BP, benzo[*a*]pyrene; (+)-*anti*-BPDE, (+)-*anti*-7,8-dihydroxy-9,10-epoxy-7,8,9,10-tetrahydrobenzo[*a*]pyrene; CDNB, 1-chloro-2,4-dinitrobenzene; GSH, glutathione; GST, glutathione *S*-transferase; GS−BPD, GSH conjugate of (+)-*anti*-BPDE; IPTG, isopropyl β-D-thiogalactopyranoside; LB medium, Luria-Bertani medium; PAHs, polycyclic aromatic hydrocarbons.

10.1021/bi9908078 CCC: $18.00
Published on Web 07/14/1999

distinct classes, namely Alpha, Mu, Pi (*19*), Theta (*20*), Sigma (*21*), Kappa (*22*), and Zeta (*23*). GST isoenzymes of the above classes exhibit overlapping but discrete substrate preferences (*18*).

Previous studies with purified rat and human GSTs have shown that while Pi class isoenzyme (GSTP1-1) is highly efficient in catalyzing the GSH conjugation of (+)-*anti*-BPDE, this diol epoxide is a poor substrate for Alpha class isoenzymes (*11*, *12*). Recently, we have characterized a novel Alpha class mouse GST isoenzyme (previously designated by us as GST 9.5) (*24*), which is exceptionally efficient toward (+)-*anti*-BPDE (*13*). For example, the catalytic efficiency (k_{cat}/K_m) of this isoenzyme toward (+)-*anti*-BPDE is approximately 74−625-fold higher than those of other Alpha class murine GSTs (mGSTA3-3 and mGSTA4-4) (*13*). Furthermore, GST 9.5 is approximately 66- and 9-fold more efficient in catalyzing the GSH conjugation of (+)-*anti*-BPDE than mGSTM1-1 (Mu class) and mGSTP1-1 (Pi class), respectively (*13*). More recently, we have demonstrated (*25*) that GST 9.5 is a dimer of Al and A2 subunit types, which differ in their primary structures by 10 amino acids. In addition, we have shown that the catalytic efficiency of recombinant mGSTA1-1 toward (+)-*anti*-BPDE is >3-fold higher than that of the recombinant mGSTA2-2 (*25*).

In the study presented here, we have used chimeric enzyme construction, molecular modeling, and site-directed mutagenesis techniques to identify the amino acid residue(s) responsible for catalytic differences between mGSTA1-1 and mGSTA2-2 toward (+)-*anti*-BPDE. Here, we report that methionine-207 and isoleucine-221 in the mGSTA1-1 structure (the corresponding amino acid residues in mGSTA2-2 are leucine and phenylalanine) are critical for its high activity toward (+)-*anti*-BPDE.

EXPERIMENTAL PROCEDURES

Materials. Restriction endonucleases and T4 DNA ligase were purchased from New England BioLabs, Inc. (Beverly, MA). Taq DNA polymerase and BL21(DE3) competent cells were obtained from Promega (Madison, WI) and Novagen, Inc. (Madison, WI), respectively. The Prep-A-Gene DNA purification kit was purchased from Bio-Rad Laboratories (Hercules, CA). Epoxy-activated Sepharose 6B, GSH, and isopropyl β-D-thiogalactopyranoside (IPTG) were obtained from Sigma (St. Louis, MO). (+)-*anti*-BPDE was procured from the National Cancer Institute, Chemical Carcinogen Reference Standard Repository (Chemsyn Science Laboratories, Lenexa, KS).

Preparation of Chimeric Constructs. Plasmids pET-lld/mGSTA1 and pET-11d/mGSTA2 containing the coding regions of mGSTA1 and mGSTA2 (*25*), respectively, were isolated from DM1 bacterial cells using standard procedures. As shown in Table 1, mGSTAl and mGSTA2 differ by 10 amino acids which are distributed in three sections (I−III) as clusters of two, three, and five amino acids, respectively. Restriction enzymes *Bgl*II, *Stu*I, and *Bam*HI were used to prepare chimeric constructs (Figure 1). To replace section I of mGSTA2 with the corresponding section of mGSTA1, plasmids pET-11d/mGSTAl and pET-11d/mGSTA2 were digested with *Bgl*II, which resulted in a small fragment (about 400 bp) and a large fragment. The small fragment of pET-11d/mGSTA1 and the large fragment of pET-11d/mGSTA2

Table 1: Amino Acid Differences between mGSTA1 and mGSTA2

section	amino acid residue	mGSTA1	mGSTA2
I	65	alanine	valine
	95	serine	threonine
II	157	isoleucine	valine
	162	valine	leucine
	169	phenylalanine	leucine
III	207	methionine	leucine
	213	glutamine	glutamic acid
	218	alanine	valine
	221	isoleucine	phenylalanine
	222	glutamine	−

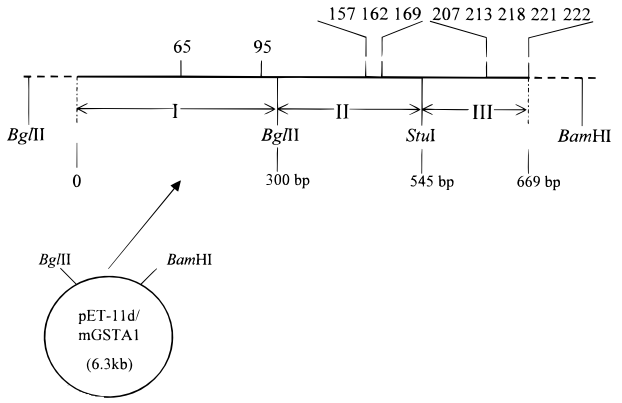

FIGURE 1: Restriction sites used to prepare chimeric constructs of mGSTA1 and mGSTA2. The solid line represents the mGSTAl cDNA insert, whereas the broken line represents the pET-l1d vector. The numbers above the line denote the positions of 10 amino acid differences between mGSTAl and mGSTA2.

were separated with a 1% agarose gel, purified using the Prep-A-Gene DNA purification kit according to the manufacturer's instructions, and ligated using T4 DNA ligase. The resultant construct contained section I of mGSTAl and sections II and III of mGSTA2. To replace section III of mGSTA2 with the equivalent section of mGSTAl, both pET-11d/mGSTA1 and pET-11d/mGSTA2 plasmids were digested with *Stu*I and *Bam*HI. The *Stu*I restriction site is located 545 bp downstream of the ATG start codon, whereas the *Bam*HI site is on the pET-11d vector downstream of the mGSTA cDNA insert location. The above digestions resulted in a small fragment (about 160 bp) containing section III of the mGSTA cDNA insert and a small portion of the vector, and a large fragment containing rest of the mGSTA cDNA insert and the vector. The small fragment of mGSTA1 was ligated with the *Stu*I−*Bam*HI large fragment from pET-11d/mGSTA2. Therefore, the resultant construct contained sections I and II of mGSTA2 and section III of mGSTA1. Preparation of a construct containing section II of mGSTA1 and sections I and III of mGSTA2 was achieved similarly using the restriction enzymes described above. The ligation mixtures containing chimeric constructs were transformed into BL21(DE3) competent cells, and the colonies were screened by plasmid analysis and GST activity determination using 1-chloro-2,4-dinitrobenzene (CDNB) as a substrate. The GST activity toward CDNB was determined by the method of Habig et al. (*26*). The protein content was determined by Bradford's method (*27*).

Molecular Modeling. Molecular modeling studies were carried out with program suites X-PLOR (*28*) and O (*29*) on an SGI Indigo2 Impact 10000 workstation. The initial model of the GSH conjugate of (+)-*anti*-BPDE (GS−BPD)

Table 2: Primers Used for Site-Directed Mutagenesis

mutation	direction	oligonucleotide sequence[a]
mGSTA1-M207L	forward a2	5′-CTCCCtTGGATGCAAAACAAA-3′
	reverse b1	5′-GCTTTCTCTGGCTGCCAG-3′
	forward a1[b]	5′-CGGATAACAATTCCCCTCTAGAA-3′
	reverse b2[b]	5′-CAGCTTATCATCGATAAGCTT-3′
mGSTA1-I221F	forward a2	5′-AGGCTTTCAAGtTTCAGTGAA-3′
	reverse b1	5′-TCCTTGCTTCTTGAATTTGTTT-3′
mGSTA2-L207M	forward a2	5′-GAAAGCCTCCCaTGGATGCAA-3′
	reverse b1	5′-TCTGGCTGCCAGGCTGTAGAAA-3′
mGSTA2-F221I	forward a2	5′-CAAGGAAGGTTTTCAAGaTTTAG-3′
	reverse b1	5′-CTTCTTCAATTTGTTTTGCATCC-3′

[a] The desired mutations in forward primer a2 are shown in lowercase. [b] Primer pair a1,b2 was common for each mutation.

was taken from the crystal structure of hGSTP1-1[V104,Al13] in complex with GS−BPD.[2] Guided with the binding mode of various GSH conjugates observed in the crystal structures of five complexes, hGSTA1-1 with *S*-benzylglutathione (*30*), hGSTAl-1 with the GSH conjugate of ethacrynic acid (*31*), hGSTA121-121 with *S*-hexylglutathione (*32*), hGSTA4-4 with iodobenzylglutathione,[3] and mGSTA4-4 with the GSH conjugate of 4-hydroxynon-2-enal,[4] the GS−BPD molecule was docked into the active site of mGSTA2-2, the crystal structure of which has been determined in the form of a mGSTA2-2·GSH[5] complex. The initial model of mGSTA1-1·GS−BPD was constructed from the initial model of mGSTA2-2·GS−BPD with the mutation-replace protocol embedded in the O graphics suite (*29*). Both complexes were built in the form of a dimeric molecule considering the fact that GSH interacts with the side chains from both subunits in the mGSTA2-2·GSH[5] complex. All the water molecules of the crystal structure were excluded in model building. The models were subjected to geometry optimization using the conjugate gradient method of Powell (*33*). The geometric parameters of Engh and Huber (*34*) were used as the basis of the force field.

Site-Directed Mutagenesis. The amino acid residues at positions 207 and 221 of mGSTA1 were replaced with the corresponding amino acids of mGSTA2 by PCR-based site-directed mutagenesis. The mGSTA1 cDNA insert in vector pET-11d was amplified by two PCRs using primer pairs a1,b1 and a2,b2, which are shown in Table 2. Forward primer a1 and reverse primer b2 were common for both mutations. The primers a1 and b2 were designed to be complementary to the vector sequence on both sides of the mGSTA cDNA insert and contained restriction sites *Xba*I and *Hin*dIII, respectively. The forward primer a2 contained the desired mutation. Reverse primers b1 for both mutations were designed to be next to the start base of the forward primer a2. The PCR mixture in a total volume of 50 μL contained 1× PCR buffer [10 mM Tris-HCl (pH 9.0), 50 mM KCl, and 0.1% Triton X-100], 3 mM $MgCl_2$, dNTPs (200 μM each), primers (2.5 μM each), 2.5 units of Taq DNA polymerase, and 20 ng of the pET-11d/mGSTA1 plasmid. PCRs were started by heating the mixture to 94 °C for 3−4 min followed by 35 cycles at 95 °C for 1 min, 60 °C for 1 min, and 72 °C for 2 min. Finally, the reaction mixture was incubated at 72 °C for 7 min. The reaction was terminated by incubation at 4 °C for more than 10 min. Two PCR products from a1,b1 and a2,b2 were gel purified and treated with PK enzyme mix from Novagen to remove nucleotide overhangs and to phosphorylate 5′-OH of the PCR products. After purification using the QIAgen PCR purification kit, the a1,b1 and a2,b2 PCR products were digested with *Xba*I and *Hin*dIII, respectively, and purified again using the QIAgen PCR purification kit. Subsequently, the two modified PCR products were ligated with the pET-11d vector which was also cut by *Xba*I and *Hin*dIII. BL2l(DE3) competent cells were transformed by the ligates, and the resulting colonies were screened by plasmid analysis and GST activity assay. The positive clones were confirmed by DNA sequencing. For double mutation, the methods that were used were the same as those for single mutations except that the template used for PCR was the single mutant mGSTA1-M207L. Mutation of amino acid residues at positions 207 and 221 of mGSTA2 with equivalents of mGSTA1 was achieved similarly except that the template used for PCR was pET-11d/mGSTA2. The PCR primers for generation of mGSTA2-L207M and mGSTA2-F221I mutants are also shown in Table 2.

Bacterial Culture and GST Purification. Bacterial clones containing the desired mGST constructs were grown overnight in Luria-Bertani (LB) medium with 100 μg/mL ampicillin. Overnight cultures were diluted 1:50 with LB medium and incubated further with shaking for 2 h at 37 °C. IPTG was then added to a final concentration of 2 mM, followed by incubation with shaking for an additional 3−4 h. Subsequently, bacteria was harvested by centrifugation at 800*g* for 5 min and kept frozen at −80 °C until they were used. Generally, bacteria from 400 to 500 mL of culture were used for GST purification. The bacterial pellet was thawed, resuspended in 50 mM Tris-HCl (pH 8.0) containing 5 mM EDTA and 50 μg/mL lysozyme, and incubated at room temperature for 15 min. The samples were sonicated to shear genomic DNA. The bacterial lysate was centrifuged at 14000*g* for 30 min. The supernatant fraction was dialyzed overnight against affinity buffer [22 mM potassium phosphate buffer (pH 7.0) containing 100 μM 2-mercaptoethanol] and subjected to GSH-linked epoxy-activated Sepharose 6B affinity chromatography. The GSH affinity chromatography was performed by the method of Simons and Vander Jagt (*35*) with some modifications described by us previously (*36*). The GST was eluted with 5 mM GSH in 50 mM Tris-

[2] X. Ji, J. Blaszczyk, B. Xiao, R. O'Donnell, X. Hu, C. Herzog, S. V. Singh, and P. Zimniak, *Biochemistry* (submitted for publication).

[3] C. M. Bruns, I. Hubatsch, M. Ridderstrom, B. Mannervik, and J. Tainer, Protein Data Bank entry 1gul (layer 1 release).

[4] B. Xiao, S. P. Singh, Y. C. Awasthi, P. Zimniak, and X. Ji, *Biochemistry* (submitted for publication).

[5] Y. Gu, B. Xiao, H. Xia, S. V. Singh, and X. Ji, manuscript in preparation.

Table 3: Specific Activities of the Wild Type and Chimeric Enzymes toward (+)-*anti*-BPDE[a]

enzyme	specific activity (nmol min^{-1} mg^{-1})
recombinant mGSTA1-1	3750 ± 280
recombinant mGSTA2-2	760 ± 20
chimeric enzyme (section I of mGSTA2-2 replaced with section I of mGSTA1-1)	760 ± 70
chimeric enzyme (section II of mGSTA2-2 replaced with section II of mGSTA1-1)	680 ± 90
chimeric enzyme (section III of mGSTA2-2 replaced with section III of mGSTA1-1)	3600 ± 150

[a] Data represent means (±SD) of at least three determinations.

HCl (pH 9.5) containing 100 μM 2-mercaptoethanol. The homogeneity of the GST preparation was checked by reverse-phase HPLC as described by us previously (*24*). The GST preparation was dialyzed against 50 mM Tris-HCl (pH 7.5) containing 2.5 mM KCl and 0.5 mM EDTA (TKE buffer) prior to kinetic studies.

Determination of GST Activity toward (+)-anti-BPDE. The GST activity toward (+)-*anti*-BPDE was determined as described by us previously (*24*, *25*). Briefly, the reaction mixture in a final volume of 0.1 mL contained TKE buffer, 2 mM GSH, 14 μg/mL GST protein, and desired concentration of (+)-*anti*-BPDE. The reaction was initiated by adding (+)-*anti*-BPDE, and the reaction mixture was incubated at 37 °C for 30 s. The reaction was stopped by rapidly mixing the solution with 0.1 mL of cold acetone, followed by extraction twice with ethyl acetate saturated with TKE buffer. The GSH conjugate of (+)-*anti*-BPDE in the aqueous phase was quantified by reverse-phase HPLC as described by us previously (*13*). A blank without the GST protein was included to account for nonenzymatic GSH conjugation of (+)-*anti*-BPDE. The GST activity was determined as a function of varying (+)-*anti*-BPDE concentration (10−120 μM) at a fixed saturating concentration of GSH (2 mM) to determine the kinetic constants. The kinetic constants were determined by nonlinear regression analysis of experimental data points using the Michaelis−Menten equation as the model.

RESULTS AND DISCUSSION

Specific Activities of the Chimeric Enzymes toward (+)-anti-BPDE. We have shown previously that mGSTA1-1 is >3-fold more efficient than mGSTA2-2 in catalyzing the GSH conjugation of (+)-*anti*-BPDE (*25*). There are 10 amino acid differences between mGSTAl and mGSTA2 (*25*), which are distributed in three sections (I−III) as clusters of two (residues 65 and 95), three (residues 157, 162, and 169), and five (residues 207, 213, 218, 221, and 222) amino acids, respectively (Table 1 and Figure 1). Section I is located in the N-terminal half of the protein, whereas the other two sections are in the C-terminal domain. Figure 2a depicts one subunit of the mGSTA2-2·GSH[5] complex highlighting the three clusters. To assess the contribution of each of the three clusters to catalytic differences between mGSTA1-1 and mGST2-2, three chimeric enzymes were generated where section I, II, or III of mGSTA2-2 was replaced with the corresponding section of mGSTA1-1. A chimeric enzyme construction technique has been used successfully by other investigators to probe the molecular mechanism of GST catalysis (*37*−*39*). As shown in Table 3, replacement of either section I or section II of mGSTA2-2 with the corresponding section of mGSTA1-1 did not increase the activity of the enzyme. On the other hand, replacement of section III of mGSTA2-2 with the corresponding section of mGSTA1-1 caused a pronounced increase in the specific activity of the enzyme. The specific activity of this chimeric enzyme was increased by about 4.7-fold compared with that of the recombinant mGSTA2-2. Moreover, the specific activity of the chimeric enzyme with section III replacement was more or less similar to that of the recombinant mGSTA1-1 (Table 3). These results clearly suggested that amino acid substitution(s) at position(s) 207, 213, 218, 221, and/or 222 may be responsible for the relatively higher activity of mGSTA1-1 toward (+)-*anti*-BPDE compared with that of mGSTA2-2.

Molecular Modeling. The model of mGSTA2-2·GS−BPD is aligned with the crystal structure of mGSTA2-2·GSH[5] in Figure 2b, which reveals that the side chains of L207 and F221 undergo significant conformational changes due to the existence of the BPD moiety. In contrast, E213 and V218 side chains do not exhibit much difference between the two complexes. The distances from the BPD moiety to the side chains are 3.8, 12.8, 11.7, and 5.6 Å for L207, E213, V218, and F221, respectively. L207 and F221 are pointing toward the BPD moiety, whereas E213 and V218 are pointing away (Figure 2b). It is therefore suggested that L207 and F221 may be catalytically more important. Because L207 interacts with the hydrophobic ring system of BPD (Figure 2b,c), it favors the protein−product interactions, and may be the protein−intermediate interactions as well. Due to the fact that the phenyl ring system of F221 interacts with the hydroxyl groups of BPD (Figure 2b,c), F221 contributes negatively to protein−product and, perhaps, protein−intermediate interactions. Instead, the two residues in mGSTA1-1 are M207 and I221 (Figure 2c). It appears that both substitutions favor protein−product interactions. Compared with L207, M207 has increased size and hydrophobicity, which improves the hydrophobic interactions between residue 207 and the ring system of BPD. I221 seems to have two advantages over F221. First, I221 is smaller than F221, which reduces the hydrophobic−hydrophilic interaction between residue 221 and the hydroxyl groups of BPD. Second, also due to the smaller size of I221, it can undergo dramatic conformational changes so that the hydrophobic CD atom interacts with the ring system of BPD, which enhances the protein−product interactions (Figure 2c). Although mGSTA1-1 has one more residue, Q222 at the C-terminus, the side chain of this residue points away from the active site as indicated by the results of molecular modeling studies (Figure 2c).

Kinetic Characterization of the Wild Type and Mutant mGSTA1-1. The results of the molecular modeling studies implied that amino acid differences between mGSTA1-1 and mGSTA2-2 at position 207 or 221, but not at position 213, 218, or 222, may account for their differential activity toward

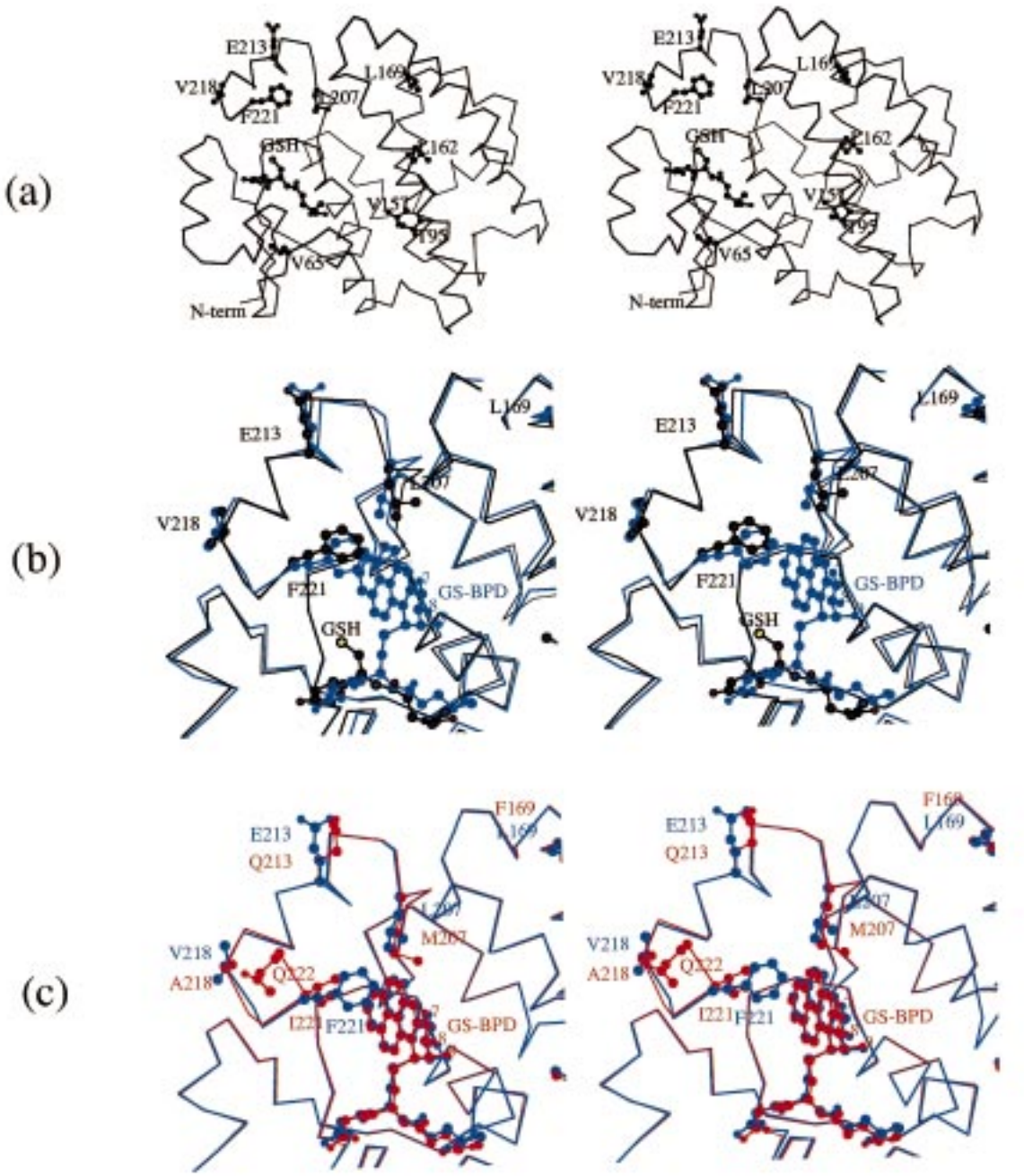

FIGURE 2: Stereoviews showing (a) one subunit of the crystal structure of mGSTA2-2·GSH,[5] (b) the comparison between the crystal structure shown in panel a and the model of mGSTA2-2·GS−BPD (blue), and (c) the alignment of the model of mGSTA2-2·GS−BPD and that of mGSTA1-1·GS−BPD (red). The atomic color scheme (carbon in black, oxygen in red, nitrogen in blue, and sulfur in yellow) is used for the side chains and GSH in the crystal structure only. In panels b and c, the hydroxyl groups at positions 7−9 of the BPD moiety are labeled. The illustration was prepared with Molscript (*45*).

(+)-*anti*-BPDE. To test this possibility, amino acid residues at positions 207 and 221 of mGSTA1-1 were replaced with the corresponding amino acids of mGSTA2-2, and the mutants were expressed in *Escherichia coli.* The wild type (recombinant mGSTA1-1 and mGSTA2-2) and the mutant enzymes were tested for their activity toward (+)-*anti*-BPDE. As shown in Figure 3, the wild type as well as the mutant enzymes adhered to Michaelis−Menten kinetics when GST activity was measured as a function of varying (+)-*anti*-BPDE concentration at a fixed saturating concentration of GSH (2 mM). Kinetic constants for the wild type and the mutant enzymes toward (+)-*anti*-BPDE are summarized in Table 4. Replacement of methionine-207 of mGSTA1-1 with leucine resulted in a ∼21% decrease in the V_{max} of the enzyme. The V_{max} of the enzyme was decreased by about 48% by substitution of isoleucine-221 of mGSTA1-1 with phenylalanine. The k_{cat} values of the mGSTAl-M207L and mGSTA1-I221F mutants were lower by about 22 and 49%, respectively, than that of wild-type mGSTA1-1. Since the V_{max} values of the mGSTA1-M207L and mGSTAl-I221F mutants were still considerably higher than those for the recombinant mGSTA2-2, we reasoned that combined interaction of amino acids at positions 207 and 221 may be important for higher catalytic activity of mGSTA1-1 because

Table 4: Kinetic Constants for the Wild Type and Mutant mGSTA1-1 toward (+)-*anti*-BPDE[a]

enzyme	V_{max} (nmol min^{-1} mg^{-1})	K_m (μM)	k_{cat} (s^{-1})	k_{cat}/K_m (mM^{-1} s^{-1})
recombinant mGSTA1-1	5360 ± 400	41 ± 9	4.5	110
recombinant mGSTA2-2	1240 ± 170	32 ± 11	1.0	31
single mutant mGSTA1-M207L	4230 ± 210	55 ± 9	3.5	64
single mutant mGSTA1-I221F	2800 ± 180	53 ± 8	2.3	43
double mutant mGSTA1-M207L/I221F	1580 ± 70	34 ± 4	1.3	38

[a] Values are means (±SD) of at least three determinations.

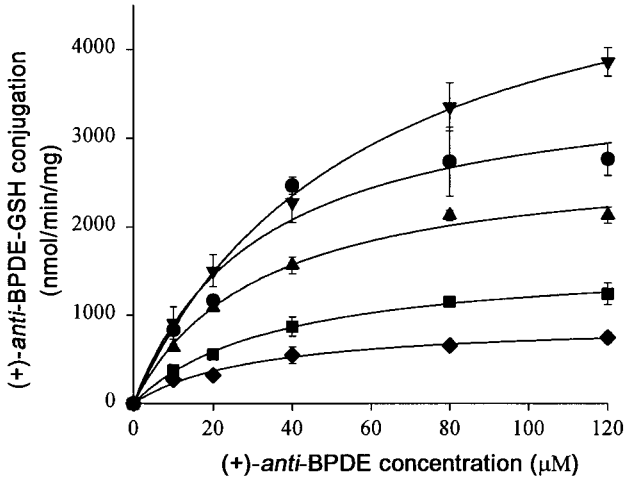

FIGURE 3: Rate of conjugation of GSH with (+)-*anti*-BPDE as a function of varying diol epoxide concentration in the presence of 14 μg/mL wild-type mGSTAl-l (▼), wild-type mGSTA2-2 (◆), single mutant mGSTAl-M207L (●), single mutant mGSTAl-I221F (▲), and double mutant mGSTA1-M207L/I221F (■). The purified wild-type and the mutant enzymes were incubated with varying concentrations of (+)-*anti*-BPDE (10−120 μM) and 2 mM GSH in TKE buffer for 30 s at 37 °C. The GSH conjugate of (+)-*anti*-BPDE was quantified by reverse-phase HPLC as described by us previously (*13*, *24*).

of enhanced hydrophobic−hydrophobic interactions and reduced hydrophobic−hydrophilic interactions between protein and the product or intermediate (see the previous section). To test this possibility, we generated a double mutant where residues at positions 207 and 221 in mGSTA1-1 were substituted with the corresponding amino acids of mGSTA2-2. The double mutation (mGSTA1-M207L/I221F mutant) resulted in about 71% reduction in the V_{max} of the enzyme. Moreover, both the V_{max} and the k_{cat} values for the mGSTAl-M207L/I221F mutant were very close to the values obtained for the wild-type mGSTA2-2.

Specific Activities of the Wild-Type and Mutant mGSTA2-2 toward (+)-anti-BPDE. The importance of the amino acid residues at positions 207 and 221 in catalytic differences between mGSTA1-1 and mGSTA2-2 toward (+)-*anti*-BPDE was further established by determining specific activities of the mutant enzymes where the above amino acid residues of mGSTA2-2 were replaced with the corresponding amino acid residues of mGSTA1-1. The specific activities of mGSTA2-L207M and mGSTA2-F221I mutants toward (+)-*anti*-BPDE (1330 ± 20 and 990 ± 33 nmol min^{-1} mg of protein^{-1}, respectively) were approximately 1.8- and 1.3-fold higher, respectively, than that of the wild-type mGSTA2-2 (760 ± 20 nmol min^{-1} mg of protein^{-1}). These results provide additional evidence for the importance of methionine-207 and isoleucine-221 in the (+)-*anti*-BPDE−GSH conjugating activity of mGSTA1-1 being higher than that of mGSTA2-2.

The results of this study clearly indicate that amino acid substitutions at positions 207 and 221 account for the observed catalytic differences between mGSTA1-1 and mGSTA2-2 toward (+)-*anti*-BPDE. The k_{cat}/K_m of the recombinant mGSTA1-1 is reduced by about 42 and 61%, respectively, by replacing methionine-207 with leucine and isoleucine-221 with phenylalanine. This is mainly due to an approximately 21 and 48% reduction in the V_{max} of the mGSTA1-M207L and mGSTA1-I221F mutants, respectively, compared with that of mGSTA1-1. The k_{cat}/K_m of mGSTA1-1 is reduced even further (about 65%) upon combined replacement of the above two amino acids. In fact, the catalytic efficiency of the double mutant mGSTA1-M207L/I221F (38 mM^{-1} s^{-1}) is more or less similar to that of the wild-type mGSTA2-2 (31 mM^{-1} s^{-1}) (Table 4).

The catalytic efficiency of mGSTA1-1 is approximately 77- and 655-fold higher than those of Alpha class murine isoenzymes mGSTA3-3 and mGSTA4-4 (*25*), respectively. The sequence of mGSTA1-1 is about 69 and 59% identical to those of mGSTA3-3 and mGSTA4-4, respectively (*18*, *25*). While the molecular basis for the remarkable difference in catalytic efficiencies between mGSTA1-1 and mGSTA3-3 or mGSTA4-4 is not clear, it is interesting to note that only mGSTA1-1 contains an isoleucine at position 221. This position is occupied by phenylalanine in mGSTA2-2 as well as in mGSTA4-4 (mGSTA3-3 is comprised of 220 amino acid residues) (*18*, *25*). On the other hand, the amino acid residue at position 207 is different among four Alpha class murine GSTs (*18*, *25*). This position is occupied by methionine in mGSTA1-1, leucine in mGSTA2-2, aspartic acid in mGSTA3-3, and proline in mGSTA4-4 (*18*, *25*). Because the side chain of residue 207 interacts with the hydrophobic ring system of BPD (Figure 2b,c), the variation from M207 in mGSTA1-1 to L207 in mGSTA1-2, to D207 in mGSTA3-3, and to P207 in mGSTA4-4 should make the isozyme less and less efficient toward (+)-*anti*-BPDE. However, the precise mechanism leading to the difference in catalytic efficiency caused by the amino acid substitutions among the four Alpha-type murine GST isoenzymes remains to be determined.

The level of amino acid sequence identity between murine GSTA1 and human GSTA1 and GSTA2 is about 75 and 78%, respectively (*25*, *40*, *41*). The amino acid residue at position 207 of human GSTA1 (methionine) is similar to that of the mouse GSTA1, whereas both mouse GSTA2 and human GSTA2 contain a leucine at position 207 (*25*, *40*, *41*). Excluding initiator methionine, murine GSTA1 contains 222 amino acids, whereas human GSTA1 and GSTA2 are comprised of 221 and 220 amino acids, respectively (*25*, *40*, *41*). The specific activity of murine GSTA1-1 is about 37- and 76-fold higher than those of hGSTA1-1 and hGSTA2-2, respectively.[6] These observations imply that neither

[6] S. V. Singh, unpublished observations.

hGSTA1-1 nor hGSTA2-2 is the functionally similar human counterpart of murine GSTA1-1. The question of whether an isoenzyme functionally related to mouse GSTA1-1 is expressed in human tissues is an interesting topic for future investigations.

It is interesting to note that the expression of Alpha class GST subunits varies considerably in tissues of A/J mice, a strain used extensively in BP-induced tumorigenesis studies (*42*). For example, mGSTA3-3 is the predominant Alpha class GST isoenzyme in A/J mice lung (*43*), which is a target organ for BP-induced tumorigenesis (*42*). On the other hand, mGSTA3-3 expression could not be detected in the forestomach (*24*), which also is a target organ for BP-induced tumorigenesis in A/J mice (*42*). Instead, the Alpha class GST activity in the forestomach of A/J mice is due to mGSTA1-2 (*24*). Since mGSTA1-2 is significantly more efficient than mGSTA3-3 in the GSH conjugation (detoxification) of (+)-*anti*-BPDE (*13*), it is not surprising that BP-induced tumor multiplicity (average number of tumor nodules per mouse) is significantly higher in the lung than in the forestomach of female A/J mice (*42*, *44*). These results suggest that GST isoenzyme composition may determine organ specificity for BP-induced tumorigenesis in mice.

In conclusion, the results of this study indicate that amino acid differences occurring at positions 207 and 221 between mGSTA1-1 and mGSTA2-2 account for their differential catalytic efficiency in the GSH conjugation of (+)-*anti*-BPDE.

ACKNOWLEDGMENT

We thank Nandita Thatte for technical assistance.

REFERENCES

1. International Agency for Research on Cancer (1983) *IARC Monographs on the Evaluation of the Carcinogenic Risk of Chemicals to Humans. Polynuclear Aromatic Compounds, Part 1. Chemical, Environmental, and Experimental Data*, Vol. 32, IARC, Lyon, France.
2. Buening, M. K., Wislocki, P. G., Levin, W., Yagi, H., Thakker, D. R., Akagi, H., Koreeda, M., Jerina, D. M., and Conney, A. H. (1978) *Proc. Natl. Acad. Sci. U.S.A. 75*, 5358−5361.
3. Slaga, T. J., Bracken, W. J., Gleason, G., Levin, W., Yagi, H., Jerina, D. M., and Conney, A. H. (1979) *Cancer Res. 39*, 67−71.
4. Sims, P., and Grover, P. L. (1974) *Adv. Cancer Res. 20*, 165−274.
5. Gelboin, H. V. (1980) *Physiol. Rev. 60*, 1107−1166.
6. Thakker, D. R., Yagi, H., Levin, W., Wood, A. W., Conney, A. H., and Jerina, D. M. (1985) in *Polycyclic Aromatic Hydrocarbons: Metabolic Activation to Ultimate Carcinogens. Bioactivation of Foreign Compounds* (Anders, M. W., Ed.) pp 177−242, Academic Press, New York.
7. Dipple, A. (1991) in *Polycyclic Hydrocarbons and Carcinogenesis. Polycyclic Aromatic Hydrocarbon Carcinogenesis: An Introduction* (Harvey, R. G., Ed.) ACS Symposium Series 283, pp 1−17, American Chemical Society, Washington, DC.
8. Yang, S. K., and Gelboin, H. V. (1976) *Cancer Res. 36*, 4185−4189.
9. Dock, L., Waern, F., Martinez, M., Grover, P. L., and Jernstrom, B. (1986) *Chem.-Biol. Interact. 58*, 301−318.
10. Thakker, D. R., Yagi, H., Levin, W., Lu, A. Y. H., Conney, A. H., and Jerina, D. M. (1977) *J. Biol. Chem. 252*, 6328−6334.
11. Robertson, I. G. C., Jensson, H., Mannervik, B., and Jernström, B. (1986) *Carcinogenesis 7*, 295−299.
12. Robertson, I. G. C., Guthenberg, C., Mannervik, B., and Jernström, B. (1986) *Cancer Res. 46*, 2220−2224.
13. Hu, X., Srivastava, S. K., Xia, H., Awasthi, Y. C., and Singh, S. V. (1996) *J. Biol. Chem. 271*, 32684−32688.
14. Hesse, S., Jernström, B., Martinez, M., Moldéus, P., Christodoulides, L., and Ketterer, B. (1982) *Carcinogenesis 3*, 757−760.
15. Fields, W. R., Morrow, C. S., Doss, A. J., Sundberg, K., Jernström, B., and Townsend, A. J. (1998) *Mol. Pharmacol. 54*, 298−304.
16. Hu, X., Herzog, C., Zimniak, P., and Singh, S. V. (1999) *Cancer Res. 59*, 2358−2362.
17. Mannervik, B. (1985) *Adv. Enzymol. Relat. Areas Mol. Biol. 57*, 357−417.
18. Hayes, J. D., and Pulford, D. J. (1995) *Crit. Rev. Biochem. Mol. Biol. 30*, 445−600.
19. Mannervik, B., Ålin, P., Guthenberg, C., Jensson, H., Tahir, M. K., Warholm, M., and Jornvall, H. (1985) *Proc. Natl. Acad. Sci. U.S.A. 82*, 7202−7206.
20. Meyer, D. J., Coles, B., Pemble, S. E., Gilmore, K. S., Fraser, G. M., and Ketterer, B. (1991) *Biochem. J. 274*, 409−414.
21. Harris, J., Coles, B., Meyer, D. J., and Ketterer, B. (1991) *Comp. Biochem. Physiol. B 98*, 511−515.
22. Pemble, S. E., Wardle, A. F., and Taylor, J. B. (1996) *Biochem. J. 319*, 749−754.
23. Board, P. G., Baker, R. T., Chelvanayagam, G., and Jermiin, L. S. (1997) *Biochem. J. 328*, 929−935.
24. Hu, X., Benson, P. J., Srivastava, S. K., Mack, L. M., Xia, H., Gupta, V., Zaren, H. A., and Singh, S. V. (1996) *Arch. Biochem. Biophys. 336*, 199−214.
25. Xia, H., Pan, S.-S., Hu, X., Srivastava, S. K., Pal, A., and Singh, S. V. (1998) *Arch. Biochem. Biophys. 353*, 337−348.
26. Habig, W. H., Pabst, M. J., and Jakoby, W. B. (1974) *J. Biol. Chem. 249*, 7130−7139.
27. Bradford, M. M. (1976) *Anal. Biochem. 72*, 248−254.
28. Brünger, A. T., and Rice, L. M. (1997) *Methods Enzymol. 277*, 243−269.
29. Jones, T. A., and Kjeldgaard, M. (1997) *Methods Enzymol. 277*, 173−208.
30. Sinning, I., Kleywegt, G. J., Cowan, S. W., Reinemer, P., Dirr, H. W., Huber, R., Gilliland, G. L., Armstrong, R. N., Ji, X., Board, P. G., Olin, B., Mannervik, B., and Jones, T. A. (1993)-*J. Mol. Biol. 232*, 192−212.
31. Cameron, A. D., Sinning, I., L'Hermite, G., Olin, B., Board, P. G., Mannervik, B., and Jones, T. A. (1995) *Structure 3*, 717−727.
32. Zeng, K., Rose, J. P., Chen, H. C., Strickland, C. L., Tu, C. P., and Wang, B. C. (1994) *Proteins: Struct., Funct., Genet. 20*, 259−263.
33. Powell, M. J. D. (1977) *Math. Prog. 12*, 241−254.
34. Engh, R. A., and Huber, R. (1991) *Acta Crystallogr. A47*, 392−400.
35. Simons, P. C., and Vander Jagt, D. L. (1977) *Anal. Biochem. 82*, 334−341.
36. Singh, S. V., Leal, T., Ansari, G. A. S., and Awasthi, Y. C. (1987) *Biochem. J. 246*, 179−186.
37. Zhang, P., Liu, S., Shan, S., Ji, X., Gilliland, G. L., and Armstrong, R. N. (1992) *Biochemistry 31*, 10185−10193.
38. Björnestedt, R., Widersten, M., Board, P. G., and Mannervik, B. (1992) *Biochem. J. 282*, 505−510.
39. Van Ness, K. P., Buetler, T. M., and Eaton, D. L. (1994) *Cancer Res. 54*, 4573−4575.
40. Tu, C.-P. D., and Qian, B. (1986) *Biochem. Biophys. Res. Commun. 141*, 229−237.
41. Rhoads, D. M., Zarlengo, R. P., and Tu, C.-P. D. (1987) *Biochem. Biophys. Res. Commun. 145*, 474−481.
42. Sparnins, V. L., Barany, G., and Wattenberg, L. W. (1988) *Carcinogenesis 9*, 131−134.
43. Hu, X., and Singh, S. V. (1997) *Arch. Biochem. Biophys. 340*, 279−286.
44. Singh, S. V., Benson, P. J., Hu, X., Pal, A., Xia, H., Srivastava, S. K., Awasthi, S., Zaren, H. A., Orchard, J. L., and Awasthi, Y. C. (1998) *Cancer Lett. 128*, 197−204.
45. Kraulis, P. J. (1991) *J. Appl. Crystallogr. 24*, 946−950.

BI9908078